Mario Thürling*, Anna Verena Witt, Robert Mau, Christoph Drobek, and Hermann Seitz

Microfluidic devices for light stimulation of cell suspensions: experimental analysis of the flow behaviour using a micro-PIV system

https://doi.org/10.1515/cdbme-2023-1021

Abstract: Photobiomodulation, the light stimulation of regenerative active cells, offers great potential for promoting tissue repair and regeneration. In this study, we show the design and fabrication of two microchannel devices for light stimulation of cell suspensions. The microchannels in the 3D-printed devices allow the uniform distribution of cells and exposure to light. Our experimental results demonstrate the ability of these microfluidic devices to improve light intake of cells in suspensions during photobiomodulation, thus enhancing the therapeutic potential.

Keywords: microfluidic device, light stimulation, cell suspension, 3D-printing, micro-PIV

1 Introduction

Regenerative medicine is an emerging field that seeks to restore or replace damaged tissues and organs using advanced biomedical technologies. Photobiomodulation, the stimulation of cells with light, has shown great potential for promoting tissue repair and regeneration [1]. Adipose derived mesenchymal stem cells (adMSCs) are a type of stem cell with therapeutic potential for a wide range of diseases and injuries. However, the efficacy of MSC-based therapies can be limited by low cell survival and retention at the site of injury. Microfluidic devices offer a promising solution to these challenges by enabling precise control of fluid flow, cell seeding, and exposure to external stimuli such as light [2].

In this paper, we describe the design and additive manufacturing of two microfluidic devices for the photobiomodulation of cell suspensions. The devices are composed of microchannels that allow for uniform distribution of cells and exposure to light of specific wavelengths and intensities. The two microchannel devices feature different flow conditions. We want to achieve an optimized light exposure to the cells and thus, an optimized light stimulation. For experimental validation of the expected flow patterns, we analysed the flow behaviour with micro-particle image velocimetry (micro-PIV).

***Corresponding author: Mario Thürling,** Microfluidics, Faculty of Mechanical Engineering and Marine Technology, University of Rostock, Justus-von-Liebig Weg 6, 18059 Rostock, Germany, e-mail: mario.thuerling@uni-rostock.de
Anna Verena Witt, Robert Mau, Christoph Drobek, Hermann Seitz, Microfluidics, Faculty of Mechanical Engineering and Marine Technology, University of Rostock, Justus-von-Liebig Weg 6, 18059 Rostock, Germany

2 Methods

2.1 Device 1: parallel flow geometry

Two designs of microfluidic devices for photobiomodulation were developed using SolidWorks (SolidWorks2021-SP03, Dassault Systèmes SolidWorks Corp, Boston, USA) as shown in Figure 1 The main dinensions are listed in table 1) .

The first microfluidic device (Figure 1, "parallel") was designed to enable the parallel flow of cells and media with a large area for illumination. The microchannel consisted of a small angled diffusor followed by a $10\,mm$ wide area. The large area for illumination was designed to be a thin channel ($h = 0.5\,mm$), which allowed for efficient exposure to light due to minimal overlap of cells in the channel. Due to the wide area, the cells and media slowed down to increase the exposure time. The design was intended to minimise mechanical stress to cells by minimising velocity gradients and detachment in the flow as cells in suspension are sensitive to stress in terms of differentiation and proliferation [3].

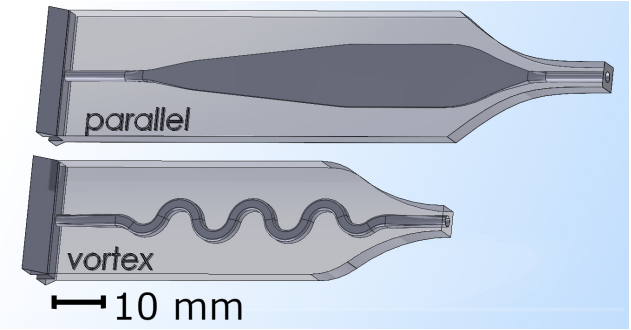

Fig. 1: Design of the microfluidic devices; top: parallel flow geometry featuring a large area for illumination; bottom: vortex generating geometry for an even stimulation of the whole sample (image generated with SolidWorks2021-SP03)

2.2 Device 2: vortex generating geometry

The second microfluidic device (Figure 1, "vortex") was designed to generate vortices within the microchannel. The microchannel consisted of an alternating series of curved channels with constant radii of curvature. This particular geometry generates a consistent secondary flow: Due to the Dean-flow effect, two tangentially opposite vortices are generated, which are perpendicular to the main flow in the microchannels axial direction [2]. These vortices cause a mixing of media and cells in the vertical direction, thus preventing the formation of parallel flow [2] [4]. This vertical mixture was thought to prevent an overexposure of cells flowing in high flow layers and underexposure of cells overlapped by other cells, allowing an even stimulation of the whole cell sample.

2.3 Manufacturing

The devices were fabricated using digital light processing (DLP). The DLP printer used was the “Vida” (Envisiontec GmbH, Gladbeck, Germany) using a XY- resolution of 73µm. In order to achieve the highest possible resolution in the Z direction, the microfluidic-devices were manufactured with the lowest possible layer height of $50\mu m$. The material used for all three samples was “E-Shell-600 resin” (Envisiontec GmbH, Dearborn, Michigan, USA), which is a biocompatible, transparent liquid resin.

After 3D printing, post processing steps were conducted. After printing, the channels were rinsed with isopropanol and post-cured in an UV curing chamber (UV Light Curing Oven, Envisiontec GmbH, Gladbeck, Germany) for 45 minutes in a beaker with pure water. To increase the clearness of the 3D printed devices, the samples were polished on both sides with a grinding machine (Saphir 520, ATMM Qness GmbH, Mammelzen, Germany, 4000 grit sandpaper). Cannulas (Precision Tips $1.65\,mm$, Nordson EFD, Ohio, US) were then glued into the inflow and outflow side of the microfluidic-devices with biocompatible two component epoxy resin (Uhu plus Endfest, UHU GmbH and Co. KG, Buehl(Baden), Germany), in order to establish a connection to the syringe pump.

2.4 Micro-PIV-Setup

To characterise the fluid flow within the microfluidic devices, we performed micro-PIV measurements using a stereo microscope (Zeiss-Stereo Discovery V20, Carl Zeiss AG, Oberkochen, Deutschland) equipped with an objective lens (Achromat S 1,0x FDW $28\,mm$). This light microscope transmits double frames inclined at a slight angle (11°), which enable depth perception. An Nd:YAG double-pulse laser (Nano S PIV, Litron Lasers Ltd, Rugby, England) with a wavelength of $532\,nm$ was used for illumination. We used two sCMOS cameras (Imager-sCMOS, LaVision, Göttingen, Germany) to capture the particle images. The double-pulse laser was synchronised with the sCMOS cameras via a programmable time unit (PTU X, LaVision, Göttingen, Germany), which controls external devices. DaVis 8.2.0 (LaVision, Göttingen, Germany) was used as software for control, evaluation and post-processing. We used a cross-correlation algorithm to calculate the velocity vectors of the tracer particles within the microchannels. The velocity data were then analysed using MATLAB (R2020a, The MathWorks, Inc., Natick, USA) to obtain the fluid flow characteristics. $10\,\mu m$ polystyrene beads (PS-FluoRot-Fi361-Particle, Micro Particles GmbH, Berlin, Germany) were suspended in deionized water and served as the tracer particles for the Micro-PIV measurement. The water resembles the cell media Dulbecco’s modified eagle’s medium (DMEM) used as carrier fluid in the operation process [5]. The polystyrene beads were chosen to replicate the adMSC in size and density as realistically as possible (average cell diameter of the adMSC 24 hours after isolation: $12.51\,\mu m$, density at $1,05\,g/cm^3$ [6]). The particles fulfilled the condition for loss-free following of the flow with a Stokes Number Stk « 1[7].

A medical syringe pump (Perfusor fm, B.Braun, Melsungen, Germany) with a delivery range of $0.1 - 1000\,ml/h$ was used to provide the low volume flow of $500\,ml/h = 1.388 \cdot 10^{-7}\,m^3/s$. The pump was connected to the microfluidic device via a supply hose and the test medium was fed into a second syringe (Omnifix LUER LOCK $50\,ml$, B.Braun, Melsungen, Germany) via a discharge hose, which served as a reservoir.

Tab. 1: Geometries of the microchannel devices in mm. The Reynolds numbers are calculated on the basis of the fluid properties, the geometric dimensions and the mean flow velocity

Name	Parallel	Vortex
Height x Width of channel	0.5 x 10	1.8 x 1.8
Reynolds Number (calculated)	25.6	77.2

3 Results and Discussion

3.1 Fabrication

Both microfluidic devices were successfully 3D printed and post-processed (see Figure 2). The devices showed no warping and the channels show high clearness as the fluid in the

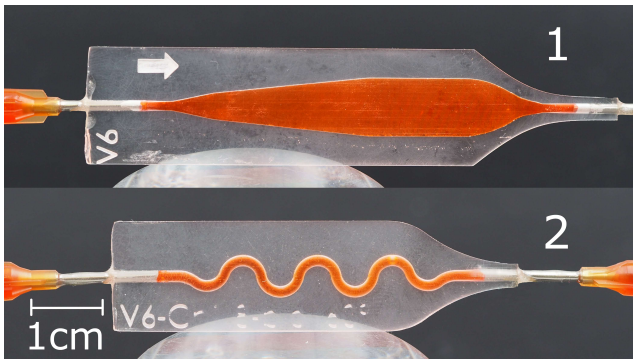

Fig. 2: Prototypes of microfluidic devices 1 and 2. Camera: Olympus OM-D E-M10 Mark III, 30 mm macro objective

channels is clearly visible. The rippled surface occurring due to the 3D-printing was completely smoothed after polishing, making them suitable for micro-PIV measurements.

3.2 PIV-results: device 1

In order to characterise the channel in terms of fluid flow, the geometry was divided into three sections: the entry section into the channel $12 < x < 20\,mm$ (Section A), the subsequent trailing area $20 < x < 32\,mm$ (Section B) and the rear channel area with maximum width $x > 43\,mm$ (Section C).

After exiting the inlet pipe (Fig. 3, start of section B), the velocity increases in the middle of the flow. This acceleration was caused by a narrowing of the profile area. After this acceleration, a deceleration due to a widening of the profile area in the diffusor occurs.

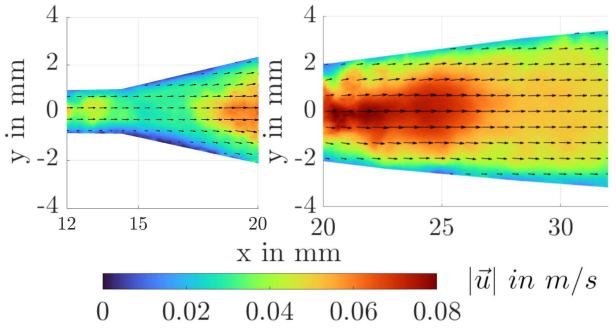

Fig. 3: Micro-PIV results of device 1 - Section A and B. u denotes the flow velocity distribution over the crossection of the device and the arrows indicate the flow direction. (image generated with MATLAB R2020a, The MathWorks Inc.)

While the flow field in the beginning of section A does not yet appear completely stationary in the middle of the flow field, the instationarities calm down towards the end of section B due to dominant viscous forces. A stationary flow field with a laminar profile has developed. The small angle of the diffusor ensures that the flow is in contact with the wall at all points and that no recirculation areas form. Otherwise, especially in the area between the inlet and the diffusor, there would be a high risk of cells remaining in the recirculation vortex, causing an overexposion or even agglomeration of these cells.

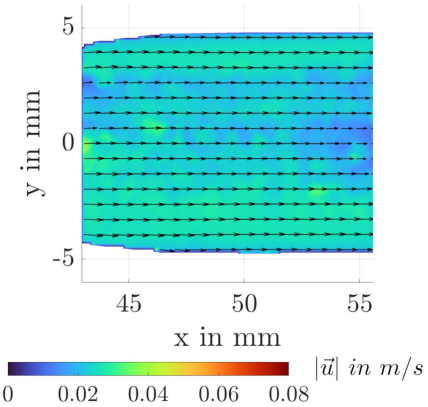

Fig. 4: Micro-PIV results of device 1 - Section C (image generated with MATLAB R2020a, The MathWorks Inc.)

In section C (see Figure 4), the fluid appears to have a stationary laminar profile with parallel streamlines over the whole section. The maximum velocity of $u_{max} = 0.043\,m/s$ occurs at the inlet edge of the section. The shear stress at the walls of the microchannels was calculated using the fluid velocity and viscosity data, and was found to be relatively low (<1 Pa).

3.3 PIV-results: device 2

In Figure 5, the velocity magnitude is shown in one complete arc. Because this arc geometry is repeated, the geometry of the vortex-channel is fully represented by this section. It can be clearly seen that the maximum velocity in the channel alternates over the cross-section from the right side in rising arcs to the left side in falling arcs.

Looking at the component u_z, it is noticeable that the velocity is positive in one half of the channel and negative in the other half. This suggests vortex formation resembling Dean flow. Following W.R. Dean, due to the curvature of a channel and the centripetal forces that occur, a pressure gradient develops which leads to the deceleration of the flow on the convex side of the curve and to the acceleration of the fluid on the concave side. The induced secondary flow is an alternating pair of vortices perpendicular to the main flow [4]. The swirling of the cell suspension prevents a stratified flow, leading to a more uniform illumination of all cells in the solution.

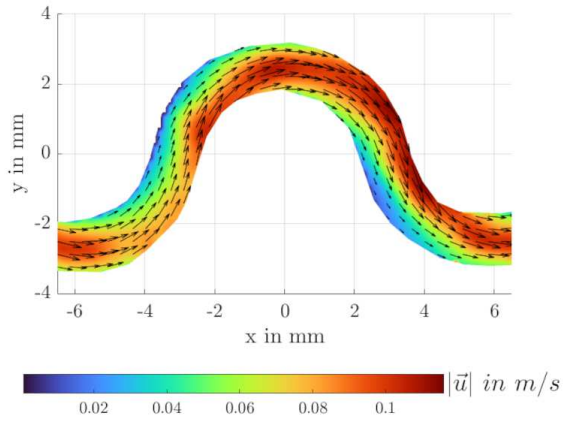

Fig. 5: Micro-PIV results of device 2 - velocity magnitude (Image generated with MATLAB R2020a, The MathWorks Inc.)

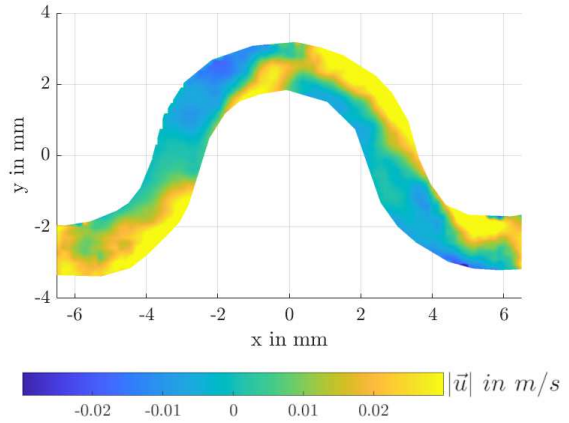

Fig. 6: Micro-PIV results of device 2 - z-component of velocity (Image generated with MATLAB R2020a, The MathWorks Inc.)

Overall, the micro-PIV measurements revealed a well-defined flow pattern within both microfluidic devices. Both devices manipulated the suspension flow in the expected behaviour without showing conspicuous flow patterns, making them both useful tools for the light stimulation of cell suspensions. The shear stress in device 1 (parallel flow geometry) is lower than in device 2 (vortex generating geometry), thus inducing less stress to the cells. On the other hand, it is possible that the cells are unevenly illuminated due to the stratified flow, which reduces the possible stimulation to the cells.

The measurements provided important insights into the flow characteristics of the microfluidic device, which can be used for the design and optimisation of future devices. However, in order to determine the actual performance and benefits of the two developed devices in terms of efficient light stimulation of cells, it is necessary to conduct further studies, especially in vitro cell studies.

4 Conclusion

In this study, we developed and 3D printed two novel microchannel devices for photobiomodulation of cell solutions. The first device generates a parallel flow with a large area for illumination, while the second device has a vortex generating channel. We characterised the devices using micro-PIV measurements and found that the vortex device produced a mixing flow profile and higher shear rates than the parallel flow device, while the parallel flow device generates a non-detaching, laminar flow through a wide illumination-window.

Overall, our study demonstrates the potential of microfluidic devices for photobiomodulation of cells. Both microfluidic devices are promising for further investigations of light stimulations and offering individual benefits. While the parallel flow device with a large area for illumination could be ideal for high-throughput, the vortex generating device appears to be ideal for an even energy input to cells.

Author Statement

This work was funded by the federal state Mecklenburg-Vorpommern and by the European Union (European Regional Development Fund), references: TBI-V-1-337-VBW-116. Conflict of interest: Authors state no conflict of interest.

References

[1] F. Ginani et al. (2015): Effect of low-level laser therapy on mesenchymal stem cell proliferation: a systematic review. Lasers Med Sci 30:2189–2194.

[2] Shamloo, Amir; Vatankhah, Parham; Akbari, Ali (2017): Analyzing mixing quality in a curved centrifugal micromixer through numerical simulation. In: Chem. Eng. Process.: Process Intensification 116, S. 9–16.

[3] Arora, Seep; Srinivasan, Akshaya; Leung, Chak Ming; Toh, Yi-Chin (2020): Bio-mimicking Shear Stress Environments for Enhancing Mesenchymal Stem Cell Differentiation. In: Curr Stem Cell Res Ther . 15 (5), S. 414–427.

[4] Dean, W. R; (1928): The stream-line motion of fluid in a curved pipe (Second paper). The London, Edinburgh, and Dublin Philosophical Magazine and Journal of Science 5, 673–695.

[5] Poon, Christine (2021): Measuring the density and viscosity of culture media for optimized computational fluid dynamics analysis of in vitro devices. In: Journal of the mechanical behavior of biomedical materials 126, S. 105024.

[6] Drobek, C.; Meyer, J.; Mau, R.; Wolff, A.; Peters, K.; Seitz, H. (2023):Volumetric mass density measurements of mesenchymal stem cells in suspension using a density meter. iScience. 26 , 105796.

[7] M. Raffel; C. E. Willert; F. Scarano; C. J. Kähler; S. T.Wereley und J. Kompenhans (2018): Particle Image Velocimetry. Cham: Springer International Publishing.